Landscape Ecol
DOI 10.1007/s10980-011-9580-8

RESEARCH ARTICLE

Topography-mediated controls on local vegetation phenology estimated from MODIS vegetation index

Taehee Hwang · Conghe Song · James M. Vose · Lawrence E. Band

Received: 5 August 2010 / Accepted: 18 January 2011

Abstract Forest canopy phenology is an important constraint on annual water and carbon budgets, and responds to regional interannual climate variation. In steep terrain, there are complex spatial variations in phenology due to topographic influences on microclimate, community composition, and available soil moisture. In this study, we investigate spatial patterns of phenology in humid temperate forest as a function of topography. Moderate-resolution imaging spectroradiometer (MODIS) vegetation indices are used to derive local patterns of topography-mediated vegetation phenology using a simple post-processing analysis and a non-linear model fitting. Elevation has the most explanatory power for all phenological variables with a strong linear relationship with mid-day of greenup period, following temperatures lapse rates. However, all other phenological variables show quadratic associations with elevation, reflecting an interaction between topoclimatic patterns of temperature and water availability. Radiation proxies also have significant explanatory power for all phenological variables. Though hillslope position cannot be adequately resolved at the MODIS spatial resolution (250 m) to discern impacts of local drainage conditions, extended periods of greenup/senescence are found to occur in wet years. These findings are strongly supported by previous field measurements at different topographic positions within the study area. The capability of detecting topography-mediated local phenology offers the potential to detect vegetation responses to climate change in mountainous terrain. In addition, the large, local variability of meteorological and edaphic conditions in steep terrain provides a unique opportunity to develop an understanding of canopy response to the interaction of climate and landscape conditions.

Keywords Vegetation phenology · MODIS · NDVI · Coweeta · Climate change

Electronic supplementary material The online version of this article (doi:10.1007/s10980-011-9580-8) contains supplementary material, which is available to authorized users.

T. Hwang (✉) · L. E. Band
Institute for the Environment, University of North Carolina at Chapel Hill, 337 W. Rosemary St., Campus Box 1105, Chapel Hill, NC 27599, USA
e-mail: h7666@email.unc.edu

C. Song · L. E. Band
Department of Geography, University of North Carolina at Chapel Hill, Saunders Hall, Campus Box 3220, Chapel Hill, NC 27599, USA

J. M. Vose
Coweeta Hydrologic Laboratory, USDA Forest Service, 3160 Coweeta Lab Rd, Otto, NC 28763, USA

Introduction

In recent decades, changes in global vegetation phenology have been associated with global-warming in a number of studies (e.g. Menzel and Fabian 1999; Zhou et al. 2001; Menzel et al. 2006) and are often

linked to the amplitude and timing of seasonal cycles of atmospheric CO_2 (Keeling et al. 1996; Myneni et al. 1997; Churkina et al. 2005), although the linkage may be locally complicated by water stress (White and Nemani 2003; Angert et al. 2005). Many of these studies have focused on climatic controls on vegetation phenology in the mid- and high-latitudes, where greater shifts in phenological patterns occur (White et al. 1997; Zhou et al. 2001; Zhang et al. 2004, 2006). Vegetation phenology in the mid- and high-latitudes is primarily controlled by temperature and photoperiod, while vegetation phenology in the tropics and in semi-arid areas is primarily controlled by seasonal rainfall (e.g. Jolly et al. 2005). A single climate factor, however, is not always sufficient to explain vegetation phenology at a given location. Rather, multiple factors act on phenology simultaneously or at different phases of vegetation development (White et al. 1997; Partanen et al. 1998).

In the humid temperate southeastern United States, although precipitation is generally plentiful, long growing season lengths and high potential evaporation can result in significant water stress during dry years in specific topoclimatic settings. Water stress is considered an important factor influencing forest community composition and biodiversity in Southern Appalachian ecosystems (Day et al. 1988). Although temperature and photoperiod are considered dominant controls of broadleaf forest phenology, water limitations may provide an important secondary influence which may increase with climate change and increased interannual hydro-climate variability. In mountain ecosystems, this may have a differential effect on different landscape positions, leading to complex spatial ecohydrological patterns. In this paper, we investigate the interaction of mountain topoclimate (temperature, radiation and water availability) on phenological response of vegetation, and implications of climate change on greenup and senescence.

Topography-related controls on vegetation phenology are not only mediated by microclimate factors, but also by species distributions, and hillslope drainage moisture gradients. Although most empirical models for vegetation phenology use climate variables (e.g. Jolly et al. 2005; Richardson et al. 2006), significant topoclimate-induced heterogeneity in canopy phenology needs to be explained by topographic factors which are easy to measure and good surrogates for microclimate and other factors. An understanding of the topography-mediated controls on vegetation phenology may therefore yield more accurate predictions of climate change effects on ecohydrological processes and understanding of ecohydrological diversity in mountain regions.

A time-series analysis of vegetation indices from global satellite images makes it possible to understand phenological signals across different spatial scales (e.g. White et al. 1997; Zhang et al. 2006; Fisher et al. 2006). Although several researchers have used field measurements to study topography-mediated controls on vegetation phenology (e.g. Richardson et al. 2006; Fisher et al. 2006; Vitasse et al. 2009), few studies have used satellite imagery for this purpose. The lack of studies using global satellite products for topography-mediated vegetation phenology is mostly due to coarse sensor spatial resolution, which may obscure fine-scale variation in phenological signals, despite their high temporal frequency.

The U.S. National Aeronautics and Space Administration (NASA) Earth Observing System currently produces a global vegetation index (VI) for the entire terrestrial earth surface at 250-m spatial resolution (MOD13Q1) every 16 days to provide a consistent measure of vegetation conditions from the Moderate resolution imaging spectroradiometer (MODIS) sensor aboard the Terra/Aqua platforms (Huete et al. 2002). MODIS land products provide more stable information on regional or continental scale vegetation phenology in both spatial and temporal domains, and have been successfully compared with field measurements (Zhang et al. 2004, 2006; Fisher et al. 2006). MODIS VI products provide more detailed information than previous global satellite products, but there is still significant sub-grid variability in topography in mountainous terrain. However, MODIS data may provide basic information on how vegetation phenology varies with topography at the hillslope scale, and which factors are dominant in controlling phenology at different phases of vegetation development.

The objectives of this study are (1) to develop a robust approach to extract phenological signals from multi-year trajectories of the 250-m MODIS NDVI, (2) to detect topography-mediated controls on local vegetation phenology at MODIS scale and validate with field measurements, and (3) to develop an understanding of how phenological patterns are

related to short length scale variations (e.g. hillslope) of topographic factors which incorporate information on microclimate, vegetation community type, and hillslope positions in mountainous terrain.

Materials and methods

Study area

This study is conducted in the Coweeta Hydrologic Lab, located in western North Carolina, USA with typical Southern Appalachian forests (Fig. 1). The Southern Appalachian forest has very diverse flora as a result of the complex terrain and consequent variability in microclimate and soil moisture (Whittaker 1956; Day and Monk 1974). Mean monthly temperature varies from 3.6°C in January to 20.2°C in July. The climate in the Coweeta Basin is classified as marine, humid temperate, and precipitation is distributed relatively even in all seasons; annual precipitation ranges from 1,790 to 2,360 mm with about a 5% increase for each 100 m increase in elevation (Swift et al. 1988). The dominant canopy species are oaks (*Quercus* spp.) and mixed hardwoods including *Carya* spp. (hickory), *Nyssa sylvatica* (black gum), *Liriodendron tulipifera* (yellow poplar), and *Tsuga canadensis* (eastern hemlock), while major evergreen understory species are *Rhododendron maximum* (rhododendron) and *Kalmia latifolia* (mountain laurel) (Day et al. 1988). Spatial distributions of forest community types in this study area are closely related to elevation, aspect, and moisture gradients (Fig. 2; Day et al. 1988), associated with distinct phenological patterns at different topographic positions.

MODIS vegetation index

With its high temporal frequency, MODIS normalized difference vegetation index (NDVI) is particularly useful to detect phenological changes. NDVI is a normalized ratio between surface reflectance in red (ρ_{RED}) and near infrared (ρ_{NIR}) portions of the electromagnetic spectrum:

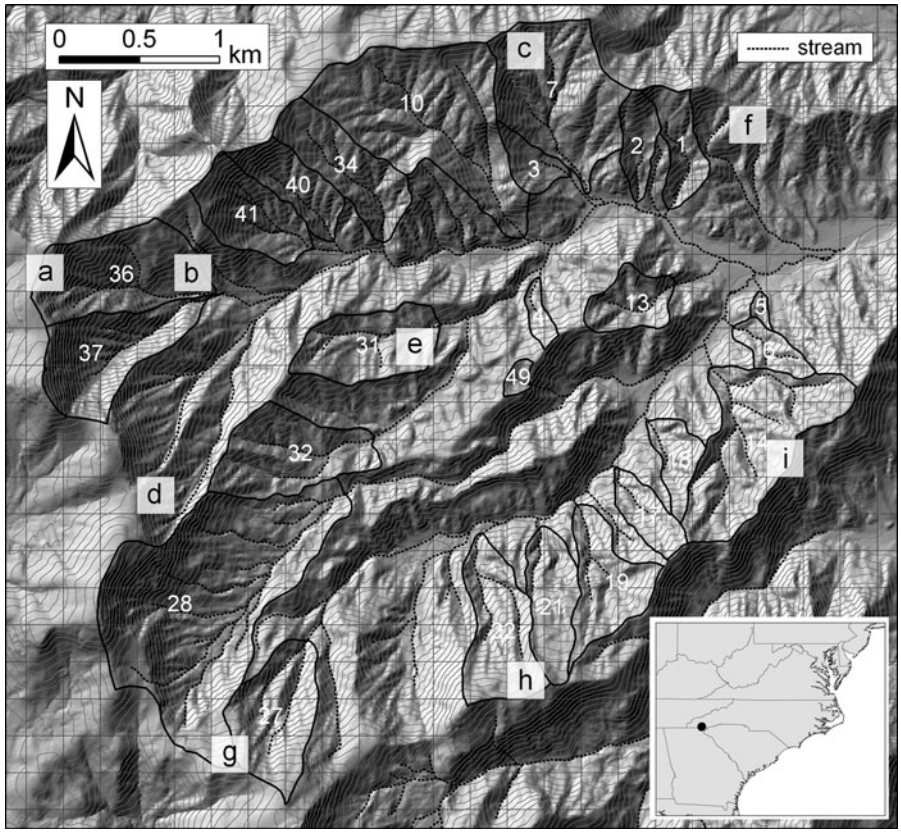

Fig. 1 A study area (Coweeta Hydrologic Lab). Grids represent the MODIS (MOD13Q1; about 250 m) pixels. *Sold lines* represent the boundaries of watersheds. *Letters* indicates the pixels for examples of filtering and fitting methods (Fig. 3)

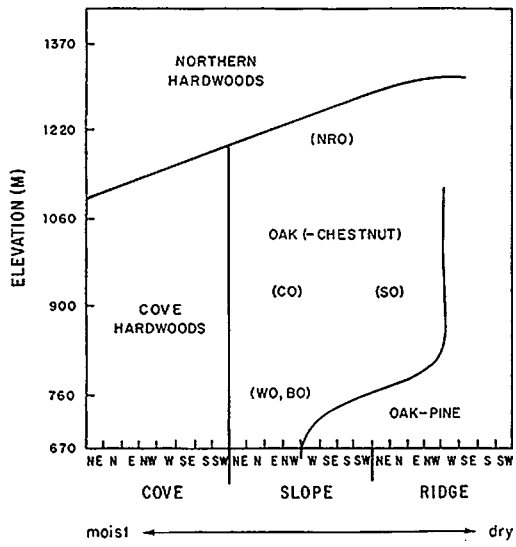

Fig. 2 A typic diagram reprinted from Day et al. (1988), which describes vegetation community types within the study area as a function of slope, aspect, elevation and hillslope positions. *BO* Black Oak, *CO* Chestnut Oak, *NRO* Northern Red Oak, *WO* White Oak. Reproduced with permission from Day et al. (1988)

$$NDVI = (\rho_{NIR} - \rho_{RED})/(\rho_{NIR} + \rho_{RED}) \quad (1)$$

NDVI has a non-linear relationship with Leaf Area Index (LAI), saturating at high LAI values (Myneni et al. 2002). This can result in significant bias including exaggerated phenological signals in low NDVI ranges, where phenological signals can be confused with understory evergreen vegetation (Fisher et al. 2006). We apply a non-linear transformation between 1-km MODIS NDVI (MOD13A2) and LAI (MOD15A2) of the study area (Fig. S3 in supplementary material) to the 250-m MODIS NDVI (MOD13Q1) to correct for the bias that the NDVI would produce for mid-points of greenup and senescence in dense humid temperate forests.

We produce the 250-m LAI dataset as MODIS data (MODIS vegetation dynamics, MODIS LAI) at 500-m or 1-km resolution strongly dampen the phenological signals between various topographic positions in complex terrain (Fig. 1). In addition, it seems that both quality control (QC) and extra QC flags cannot detect unqualified data efficiently due to substantial spatial variation in microclimate in this humid and mountainous area.

In the production of the 250-m NDVI from 2001 to 2008, both good and marginal VI values are chosen based on pixel reliability, a parameter recently added to MODIS VI products (collection 5) (Didan and Huete 2006). The day of composite at each pixel is also retrieved to get the exact acquisition date during each composite period. Two experimental watersheds (WS01, WS17; Fig. 1), where white pine (*Pinus strobus* L.) was planted in 1957 and 1956, are excluded from the statistical analysis due to distinct phenological patterns featured by coniferous forests.

Post-processing analysis

A two-step filtering approach is developed to identify occasional negative or positive spikes not indicated by the quality assurance flags. Most spikes are negative forms due to remnant cloud cover, aerosols, or cloud shadow, all of which tend to decrease the NDVI values (Didan and Huete 2006). First, unqualified data points are eliminated from the 8-year historical phenological trajectories (2001–2008) assuming that temporal phenological patterns of forest-based ecosystems are consistent and that interannual variations are relatively small compared to seasonal variations. From historical trajectories of estimated MODIS LAI as a function of day of year at each pixel (Fig. 3), we group all data points occurring within 16 days before and after at each data point. If a data point is classified as an outlier beyond ends of the group whiskers, defined as 1.5 times the interquartile range from lower and upper quartiles, it is excluded from the further analysis. By including the 16-days before and after LAI values in this outlier-exclusion process, we can account for interannual variations in phenological changes, especially during the transition periods, and obtain a statistically significant number of data points. Second, we use the modified Best Index Slope Extraction (BISE) method to remove remnant spikes (Lovell and Graetz 2001).

Our simple filtering technique is very effective in excluding unqualified data points from the time-series of transformed MODIS LAI values for selected pixels at different topographic positions in the study area (Fig. 3). The percentages of filtered-out values in the time series of MODIS LAI are usually around 10% (Fig. 4d), most of which are in the summer season. This outlier-exclusion method from historical trajectories is especially useful for rare positive spikes and

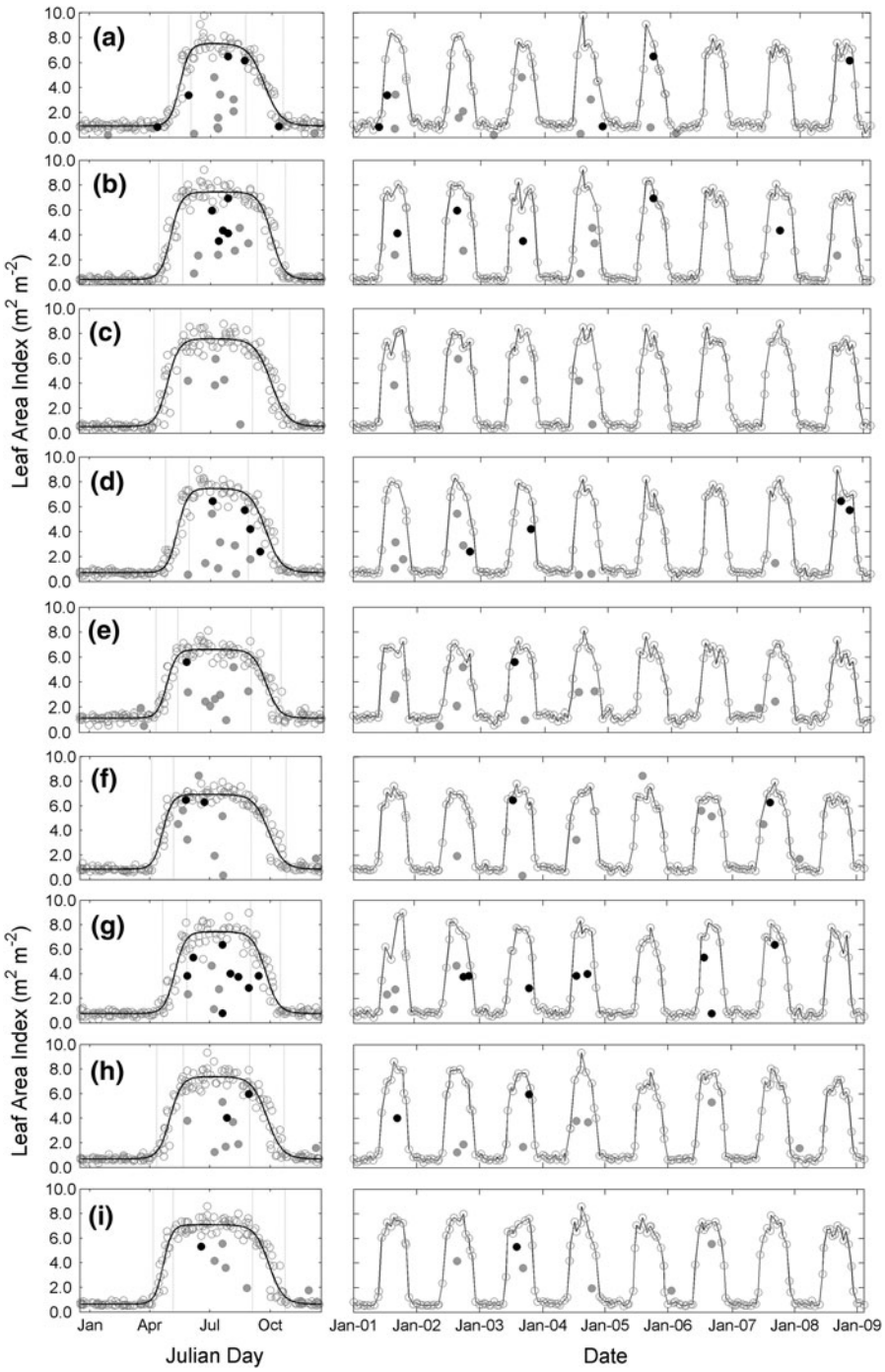

Fig. 3 Examples of two-step filtering and non-linear fitting with the difference logistic function from 8-year historical trajectories (*left column*) and time-series (*right column*) of estimated LAI at selected MODIS pixels ((a–i); Fig. 1). *Grey* and *black dots* represent filtered values by the outlier exclusion analysis and the modified BISE methods, respectively. *Vertical lines* are phenological transition dates (supplementary material)

consecutive false data points from composite periods. It also works well around transition periods by allowing flexibility in interannual phenological variations.

A phenology model for multi-year NDVI datasets

A common phenology model for temporal MODIS VI or LAI values is the single logistic function

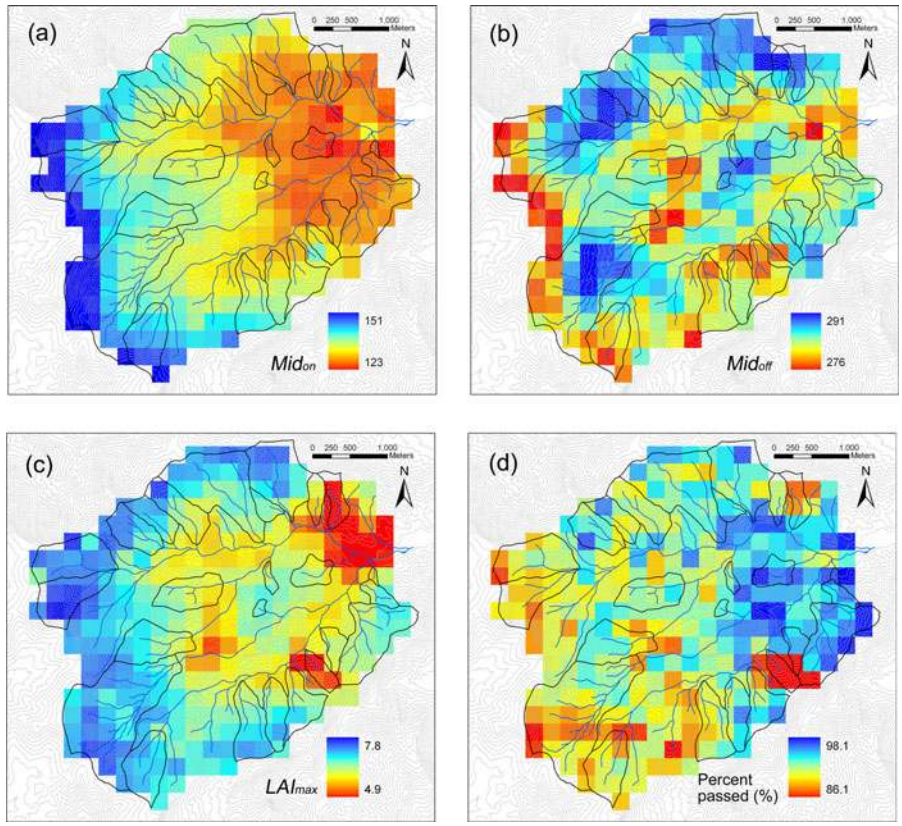

Fig. 4 Spatial patterns of phenological variables, **a** Mid_{on} (DOY), **b** Mid_{off} (DOY), **c** LAI_{max} (m^2 m^{-2}), and **d** percent passed (%) by the suggested filtering technique within the study area

(Zhang et al. 2004), generally used for a single growth or senescence phase. Phenological changes in forest ecosystems, however, are quite periodic with a single mode of growth and senescence per year. We therefore use the difference logistic function to develop a functional representation of a 1-year period from multi-year LAI records (Fisher et al. 2006):

$$y(t) = \left(\frac{1}{1+e^{a+bt}} - \frac{1}{1+e^{a'+b't}}\right)c + d \qquad (2)$$

where a and b are fitting parameters for the greenup period, a' and b' are those for the senescence period, d is the minimum or background NDVI or LAI value, and c is the difference between maximum and minimum NDVI or LAI. To extract average topography-mediated vegetation phenology, we pooled MODIS LAI data from all years together to estimate the model parameters, assuming the interannual variation in phenology is a secondary source of variation. And then, temporal patterns of MODIS LAI as a function of DOY (day of year) can be differentiated by topographic positions (Fig. 3).

Following Zhang et al. (2004), phenological transition dates (greenup, maturity, senescence, and dormancy onsets) in the logistic model can be determined from the local minima and maxima for the rate of curvature change, the derivative of the curvature of the logistic function (Eq. 3 in Zhang et al. 2004). Analytical solutions are solved for these transition dates to calculate the length of growth and senescence periods ($Length_{on}$ and $Length_{off}$; Table 1), which characterize the local phenological patterns of the study area (supplementary material). The mid-day of leaf greenup/senescence periods (Mid_{on} and Mid_{off}; Table 1; Fig. 4) are also used for the statistical analysis in this study, equivalent to inflection points for the difference logistic function (e.g. White et al. 1997, 2002; Fisher et al. 2006).

Topographical variables

Phenological variables from MODIS LAI are related to basic topographic variables at the MODIS scale (250 m). Elevation (*elev*) data are aggregated from North Carolina LIDAR digital elevation data (about

Table 1 Summary of phenological and topographic variables

Abbreviation	Description	Unit	Equation or reference
Phenological variables			
Mid_{on}	Mid-day of greenup period	DOY	$-a/b$ from Eq. 2
Mid_{off}	Mid-day of senescence period	DOY	$-a'/b'$ from Eq. 2
$Length_{on}$	Length of greenup period	Days	Supplementary material
$Length_{off}$	Length of senescence period	Days	Supplementary material
LAI_{min}	Fitted minimum LAI value	Unitless	d from Eq. 2
LAI_{max}	Fitted maximum LAI value	Unitless	$c+d$ from Eq. 2
Topographic variables			
elev	Elevation	m	http://www.ncfloodmaps.com
taspect	Transformed aspect	Unitless	Beers et al. (1966)
PRR_g	Potential relative radiation (*PRR*) for greenup season	Unitless	April, May
PRR_f	Potential relative radiation (*PRR*) for senescence season	Unitless	October, November
topidx	Topographic wetness index	Unitless	Eq. 3

6.1-m resolution). From these aggregated elevation datasets, aspect and slope are calculated at the same spatial resolution. To create a more direct measure of radiation load for statistical analysis, aspect is transformed into a number ranging from −1 (northeast-facing) to 1 (southwest-facing) (*taspect*) with a cosine function (Beers et al. 1966).

In order to account for combined slope/aspect with solar geometry on incoming radiation, potential relative radiation (*PRR*; Pierce et al. 2005) is computed. To represent the soil water availability along hillslope gradient, the topographic wetness index (*topidx*; Beven and Kirkby 1979) is calculated with the *D*-infinity ($D\infty$) method (Tarboton 1997):

$$topidx = \ln\left(\frac{a}{\tan\beta}\right) \quad (3)$$

where a is upslope contributing area per unit contour length and β is local slope. The *topidx* variable is calculated at the original LIDAR resolution, and then averaged up to the 250-m resolution, because detailed hydrological variations can be lost when wetness index is calculated at the MODIS scale in contrast to aspect and slope. All phenological and topographic variables are summarized in Table 1.

Interannual variations between wet and dry years

As the range of topographic wetness index is significantly reduced at the MODIS scale, it is difficult to detect the topography-mediated controls on vegetation phenology in terms of hillslope position. For this reason, we compare phenological variables between very wet and dry years to determine whether soil moisture status has a significant effect on vegetation phenology. In this region, we have experienced both exceptionally wet and dry conditions since 2000. Phenological signals are analyzed from two extremely dry years (2001 and 2007) and two extremely wet years (2003 and 2005). Annual precipitations in wet years (2,109 and 2,074 mm) were at least 15% higher than the 74-year average annual precipitation at the base station (RG06, 1,780 mm), while the precipitations in dry years (1,395 and 1,213 mm) were more than 20% lower. Using phenological signals from years with extreme moisture conditions, we may attribute phenological differences to interannual variations of moisture condition, minimizing the effect of interannual variations of other climate variables (e.g. temperature, radiation etc.). We also explore how major topography-mediated controls on vegetation phenology change between wet and dry years, and how we can interpret such changes with respect to the role of moisture status for vegetation phenology.

Statistical analysis

A multiple regression analysis is used to relate phenological variables to topographic variables. We

do not include topographic slope in this analysis, as there is a significant positive correlation between slope and elevation in this study area (Pearson correlation coefficients; $R = 0.592$, $P < 2\times10^{-16}$). A Pearson correlation matrix between all explanatory and response variables indicates that there is no other significant correlation among explanatory variables ($P > 0.01$; not shown here) except for the correlation between radiation proxies (*taspect* and *PRR*). Therefore, only one radiation proxy is used for the multiple regression analysis at a time, *taspect* (*model 1*) or seasonal *PRR* (*model 2*) (Table 3). Quadratic terms for each of the explanatory variables are included, as well as interaction terms. In addition, LAI_{min} effectively represents the amount of evergreen vegetation which has distinct phenological patterns compared with deciduous broadleaf forests. To explain the effect of evergreen vegetation in phenological signals, LAI_{min} is added into explanatory variables.

The analysis of covariance technique is incorporated to test the inequality of regression lines (for separate lines) between topographic controls on vegetation phenology for wet and dry years. It tests whether the responses of the independent variables (phenological variables) are different between groups as a linear function of the predictor variables (topographic variables). Only major linear topographic controls on vegetation phenology are tested to simplify this procedure.

Field measurements of vegetation phenology at different topographic positions

Although we do not have concurrent field measurements of vegetation phenology with MODIS images, we derived indirect estimates of phenological dynamics from light transmittance data collected at six different sub-watersheds within the study area in 1989. The sub-watersheds are sampled from low, middle, and high elevation regions with opposite south and north facing slopes (Table 2; Fig. 1). These phenological observations at different topographic positions help to validate the major topographic controls on vegetation phenology estimated from MODIS datasets.

Light transmittance measurements were made with a portable Sunfleck Ceptometer (Decagon Devices, Pullman, WA, USA) and were previously described by Vose and Swank (1990). Light interception ratios are used (i.e., below-canopy/open) to estimate seasonal LAI dynamics (Fig. S4 in supplementary material). At each location, photosynthetically active radiation (PAR) was measured at ten permanently marked below-canopy plots. The above canopy PAR is the mean of open sky measurements before and after the measurement of PAR under the canopy. We use the highest value for each watershed over the sample period as our estimates of peak seasonal LAI, and all other values are relative to the peak LAI based on PAR interception percentages to compare normalized phenological features between locations. Mid-days of greenup/senescence periods (Table 2) are estimated from these measurements by interpolation between adjacent points, as suggested by White et al. (1997).

Table 2 Topographic and phenological features from field measurements in different plot locations for 1989

Aspect	Watershed ID[a]	Elevation (m)	Mid_{on} (DOY)	Mid_{off} (DOY)
South	WS02	700	122	309
	WS34	1000	132	289
	WS36	1300	145	282
North	WS14	730	121	302
	Near WS22	884	135	280
	WS27	1463	142	275

[a] Shown in Fig. 1

Results

Topographical controls on local vegetation phenology

Summaries of the multiple regression analyses are shown in Table 3. For both models, *elev* usually has the most explanatory power for all phenological variables. However, Mid_{on} exhibits a linear relationship with *elev*, while the other three phenological variables (Mid_{off}, $Length_{on}$, and $Length_{off}$) exhibit quadratic responses in both models. Radiation proxies (*taspect* and *PRR*) are also significant for phenological variables usually as a linear relationship with *taspect*, and linear or quadratic relationships with seasonal *PRR*. For both models, LAI_{min} is highly significant for two mid-day phenological variables,

Table 3 Summaries of multiple regression models ($n = 252$)

	Model 1 (*taspect*)	Model 2 (*PRR*)
Mid_{on}	Equation: $Mid_{on} \sim elev + topidx + taspect + LAI_{min} + elev*taspect$ Coefficients *elev*: $3.40\times10^{-2} \pm 4.17\times10^{-4}$ ($P<2\times10^{-16}$) *topidx*: 1.57 ± 0.18 ($P = 1.02\times10^{-15}$) *taspect*: -3.00 ± 0.63 ($P = 2.90\times10^{-6}$) LAI_{min}: 4.86 ± 0.38 ($P<2\times10^{-16}$) *elev*taspect*: $3.53\times10^{-3} \pm 6.4\times10^{-4}$ ($P = 8.54\times10^{-8}$) Multiple R^2: 0.972	Equation: $Mid_{on} \sim elev + topidx + PRR_g + LAI_{min}$ Coefficients *elev*: $3.35\times10^{-2} \pm 4.2\times10^{-4}$ ($P<2\times10^{-16}$) *topidx*: 1.51 ± 0.19 ($P = 9.95\times10^{-14}$) PRR_g: $1.63\times10^{-3} \pm 3.8\times10^{-4}$ ($P = 2.08\times10^{-5}$) LAI_{min}: 4.45 ± 0.39 ($P<2\times10^{-16}$) Multiple R^2: 0.969
Mid_{off}	Equation: $Mid_{off} \sim elev^2 + elev + taspect + LAI_{min}$ Coefficients $elev^2$: $-2.74\times10^{-5} \pm 2.2\times10^{-6}$ ($P<2\times10^{-16}$) *elev*: $5.16\times10^{-2} \pm 4.8\times10^{-3}$ ($P<2\times10^{-16}$) *taspect*: 1.16 ± 0.14 ($P = 4.39\times10^{-15}$) LAI_{min}: -9.10 ± 0.52 ($P<2\times10^{-16}$) Multiple R^2: 0.751	Equation: $Mid_{off} \sim elev^2 + elev + PRR_f^2 + LAI_{min}$ Coefficients $elev^2$: $-2.75\times10^{-5} \pm 2.2\times10^{-6}$ ($P<2\times10^{-16}$) *elev*: $5.21\times10^{-2} \pm 4.7\times10^{-3}$ ($P<2\times10^{-16}$) PRR_f^2: $3.61\times10^{-7} \pm 4.0\times10^{-8}$ ($P<2\times10^{-16}$) LAI_{min}: -9.04 ± 0.51 ($P<2\times10^{-16}$) Multiple R^2: 0.761
$Length_{on}$	Equation: $Length_{on} \sim elev^2 + elev + taspect + LAI_{min}$ Coefficients $elev^2$: $-3.39\times10^{-5} \pm 5.6\times10^{-6}$ ($P = 6.74\times10^{-9}$) *elev*: $7.78\times10^{-2} \pm 1.23\times10^{-2}$ ($P = 1.31\times10^{-9}$) *taspect*: -2.60 ± 0.36 ($P = 3.23\times10^{-12}$) LAI_{min}: -4.43 ± 1.33 ($P = 0.00096$) Multiple R^2: 0.366	Equation: $Length_{on} \sim elev^2 + elev + PRR_g^2 + LAI_{min}$ Coefficients $elev^2$: $-3.25\times10^{-5} \pm 5.3\times10^{-6}$ ($P = 4.11\times10^{-9}$) *elev*: $7.26\times10^{-2} \pm 1.17\times10^{-2}$ ($P = 2.23\times10^{-9}$) PRR_g^2: $-1.50\times10^{-6} \pm 1.6\times10^{-7}$ ($P<2\times10^{-16}$) LAI_{min}: -4.30 ± 1.24 ($P = 0.00063$) Multiple R^2: 0.435
$Length_{off}$	Equation: $Length_{off} \sim elev^2 + elev + taspect$ Coefficients $elev^2$: $4.25\times10^{-5} \pm 5.7\times10^{-6}$ ($P = 1.74\times10^{-12}$) *elev*: $-9.01\times10^{-2} \pm 1.24\times10^{-2}$ ($P = 4.70\times10^{-12}$) *taspect*: 1.18 ± 0.36 ($P = 0.0012$) Multiple R^2: 0.216	Equation: $Length_{off} \sim elev^2 + elev + PRR_f$ Coefficients $elev^2$: $4.23\times10^{-5} \pm 5.7\times10^{-6}$ ($P = 2.50\times10^{-12}$) *elev*: $-8.94\times10^{-2} \pm 1.24\times10^{-2}$ ($P = 7.56\times10^{-12}$) PRR_f: $1.82\times10^{-3} \pm 5.9\times10^{-4}$ ($P = 0.0021$) Multiple R^2: 0.213

whereas *topidx* has some explanatory power only for Mid_{on}. All interaction and quadratic terms other than *elev*taspect*, $elev^2$, and PRR^2 are insignificant for both models. Introducing the seasonal *PRR* (PRR_g or PRR_f) as a radiation proxy resulted in some improvement in model performance (R^2) for Mid_{off} and $Length_{on}$ (Table 3). Moreover, 95% confidence intervals for the coefficients of the remaining independent variables ($elev^2$, *elev*, and *topidx*) overlap significantly for both models, indicating that the choice of radiation proxy has minimal influence on the relationships between other topographic and phenological variables.

Mid_{on} is delayed by about 3.4 days for every 100 m increase in elevation (Table 3; Figs. 4a, 5a). This delay with elevation is close to Hopkins' Law which states the onset of spring is delayed by 1 day with 30 m increase in elevation (Hopkins 1918). It is interesting to note that the fitted quadratic lines between elevation and phenological variables show very similar ranges of the inflection points from the 1,100–1,200 m elevation bands (Fig. 5), the transition zone from the Southern Appalachian forests to the Northern Hardwood forests (Fig. 2).

Both radiation proxies show significant positive relationships with two senescence variables (Mid_{off}

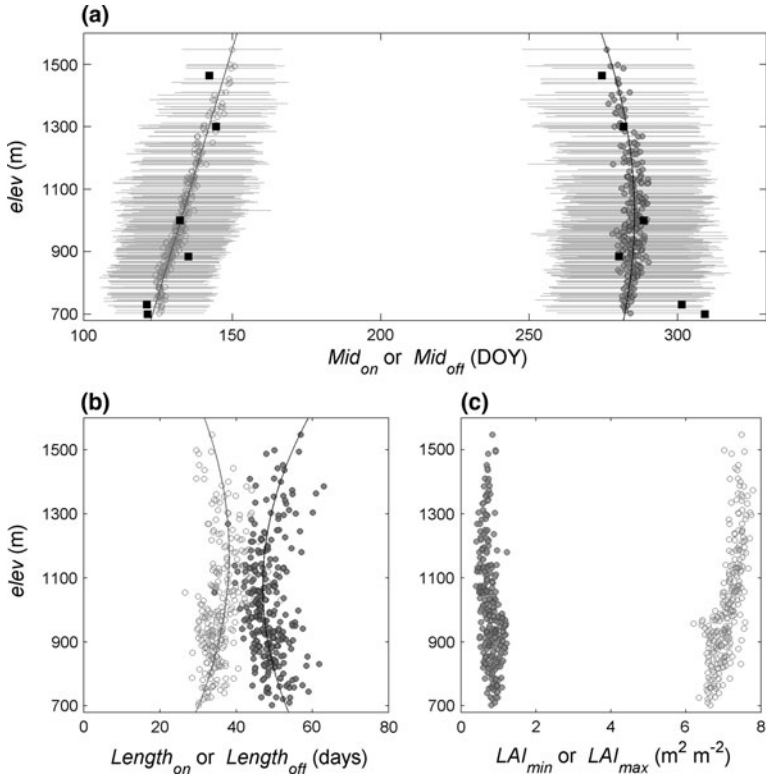

Fig. 5 Elevational controls on **a** Mid_{on} (*open*) and Mid_{off} (*filled*), **b** $Length_{on}$ (*open*) and $Length_{off}$ (*filled*), and **c** LAI_{max} (*open*) and LAI_{min} (*filled*). *Horizontal bars* represent $Length_{on}$ and $Length_{off}$. *Filled black square* points represent Mid_{on} and Mid_{off} estimated from field Ceptometer measurements (Table 2)

and $Length_{off}$), and a significant negative relationship with $Length_{on}$ (Table 3; Fig. 6). However, they show weak mixed effect on Mid_{on}, which depends on inclusion of the interaction term with *elev* (Table 3). About 2.3-day delay in Mid_{off} is indicated on south-facing slopes as compared to north-facing slopes (Figs. 4b, 6b). $Length_{on}$ on south-facing slopes is about 5.2 days shorter than on north-facing slopes, whereas $Length_{off}$ is about 2.4 days longer (Table 3; Fig. 6). Mid_{on} is also delayed by about 1.6 days for every unit increase in *topidx* (Table 3).

Seasonal vegetation dynamics at different topographic positions from PAR measurements

Seasonal dynamics of observed LAI and estimated phenological features at different topographic locations are summarized in the supplementary material and Table 2. Mid_{on} values are between DOY 120 and 145, while Mid_{off} values are scattered around DOY 290. In general, delayed greenup and early senescence are observed as elevation increases (Table 2; Fig. 5a). A simple linear regression between elevation and field estimated Mid_{on} (Table 2) indicates that about 3.0 day delays with every 100 m elevation increases ($R^2 = 0.843$). Even though this is a result from a single year (1989), it is similar to the sensitivity of Mid_{on} to elevation estimated from MODIS LAI (Fig. 5a). The quadratic response of Mid_{off} to elevation gradients appear to be consistent with the four Ceptometer measurement sites (Fig. 5a), but the lowest two sites have significantly delayed senescence.

Field estimated Mid_{on} does not show significant difference between south- and north-facing slopes within the same elevation region, whereas Mid_{off} is observed about 8-day earlier in north-facing slopes for all elevation regions (Table 2). This difference in Mid_{off} between north- and south-facing slopes is significantly larger than estimated from the 8-year MODIS LAI (Table 3). It is mainly because the phenological responses to radiation proxies at the MODIS scale may be mitigated due to the scale variance nature of radiation proxies between fine and coarse spatial resolutions (supplementary material).

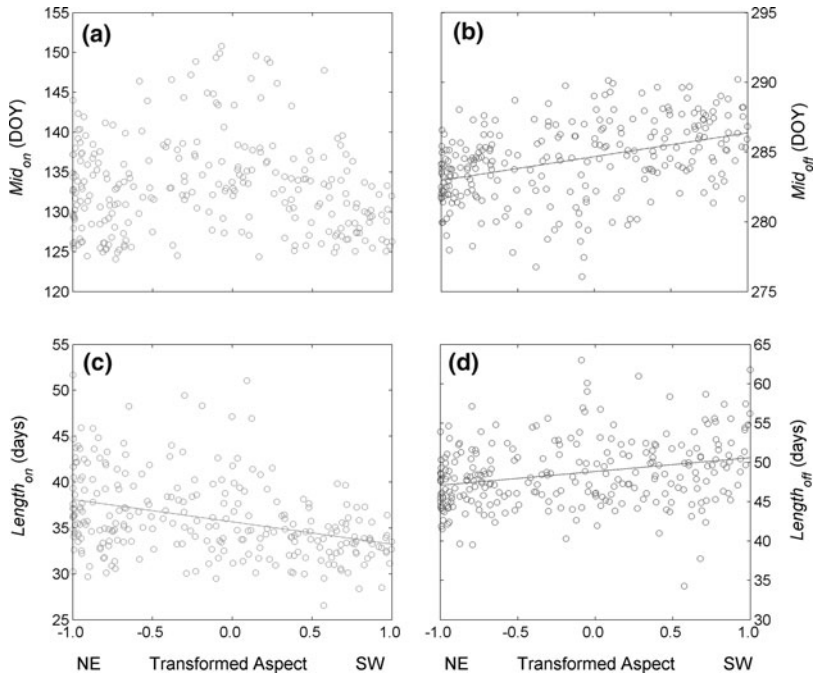

Fig. 6 Aspect controls on **a** Mid_{on}, **b** Mid_{off}, **c** $Length_{on}$, and **d** $Length_{off}$. NE and SW represent northeast and southwest facing slopes

Vegetation phenology between wet versus dry years

Scatter plots of six phenological variables (Table 1) between wet and dry years are presented in Fig. 7. Overall, there is no significant difference for either mid-day variables, though greenup is occasionally delayed in wet years at mid- and high-elevation regions (Fig. 7a). Both length variables, however, are significantly larger in wet years than in dry years at most pixels with $Length_{off}$ exhibiting greater increases (Fig. 7c, d). LAI_{max} for wet years are higher than those for dry years (Fig. 7f) especially in low LAI ranges, while fitted LAI_{min} are similar for wet and dry years (Fig. 7e).

Differences in major topography-mediated controls (*elev* and *taspect*) on two phenological length variables between wet and dry years are shown in Fig. 8. These controls on $Length_{on}$ and $Length_{off}$ show clear shifts between wet and dry years, while generally preserving their trends. Parallel shifts between wet and dry years are shown in *taspect* controls (Fig. 8b, d). The analysis of covariance test for separate lines shows that the slopes of the regression lines are not significantly different between wet and dry years ($P > 0.1$), indicating that *taspect* controls on the two phenological length variables do not vary substantially with interannual variations in moisture condition. In contrast, *elev* controls on the two variables do vary substantially between wet and dry years. Though *elev* controls on $Length_{on}$ show mixed signals, the differences between wet and dry years are smallest in low-elevation ranges (Fig. 8a). The differences in $Length_{off}$ between wet and dry years are smallest in mid-elevation ranges and largest in high- and low-elevation ranges (Fig. 8c) such that in wet years more extended senescence periods occur in high- and low-elevation ranges.

Discussion and conclusions

Elevational controls on vegetation phenology

This study quantifies how local vegetation phenology is mediated by topographic factors, closely related to microclimate variation, vegetation community type, and soil water availability in the study area. In particular, elevation is a primary factor to characterize topography-mediated phenological features, associated with environmental temperature lapse rate (Bolstad et al. 1998) and orographic precipitation increases (Swift et al. 1988). Mid_{on} is a strong linear

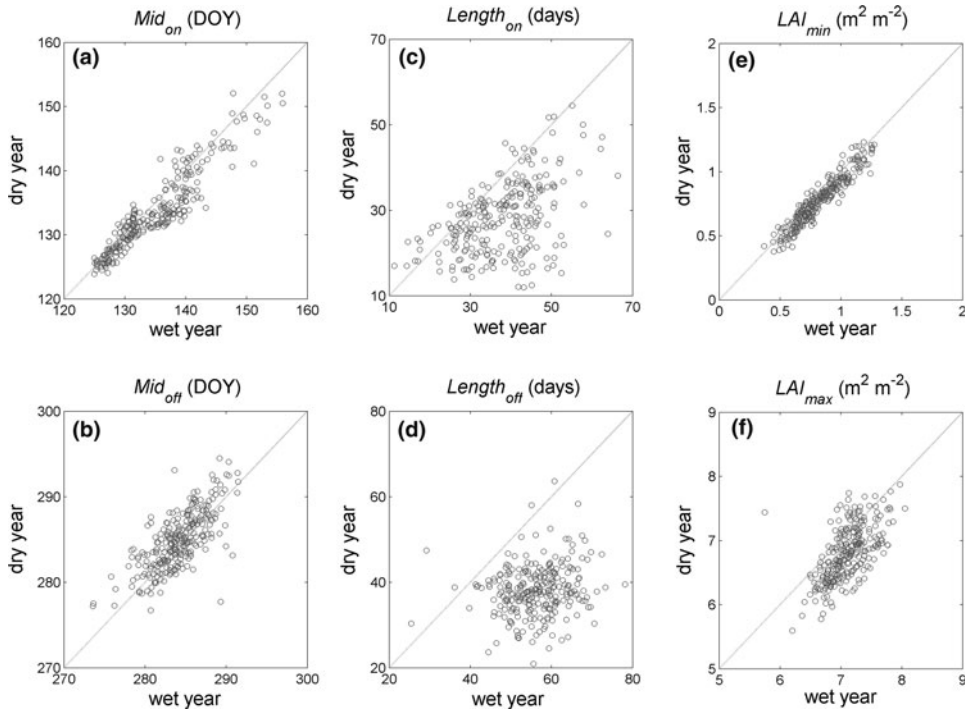

Fig. 7 Scatter plots of six phenological variables between extremely wet (2003, 2005) and dry (2001, 2007) years. **a** Mid_{on}, **b** Mid_{off}, **c** $Length_{on}$, **d** $Length_{off}$, **e** LAI_{min}, and **f** LAI_{max}

function of elevation, closely following the general empirical trend. This is induced by the dominant temperature effect on on-set of spring, especially daily minimum temperature. This is also strongly supported by field measurements at different topographic locations within the study site.

However, temperature effects alone cannot explain the quadratic responses of other three phenological variables to elevation (Fig. 5), which can be explained by combined effects with orographic precipitation patterns. Earlier senescence in the low-elevation region results from increased plant water stress caused by lower precipitation and higher potential evapotranspiration. Delayed senescence in the mid-elevation region is related to higher water availability and vegetation density following orographic precipitation increases with elevation (Figs. 4c, 5c). LAI_{max} shows increased vegetation density along the elevational gradient up to 1,200 m, correlated not only to increased water availability but also to increased wet deposition of nitrogen following precipitation (Knoepp et al. 2008). The increase of LAI_{max} may be also partially due to the increase of NDVI by the transition into the Northern Hardwood forests at higher elevation, which usually have higher near infrared reflectance. Higher LAI_{max} is also relevant to longer $Length_{on}$ at mid-elevation regions (Fig. 5b).

However, the quadratic response of Mid_{off} shows a significant deviation in the lowest two field measurement sites (Fig. 5a). The elevational control on Mid_{off} may fluctuate more interannually than that on Mid_{on} because it is related not only to interannual variability of temperature but also to that of precipitation. The year of field measurements (1989) was extremely wet due to tropical storm Allison in July and hurricane Hugo in September, so total annual precipitation amounted to 2,341 mm at low elevation (RG06; 685 m) and 3,088 mm at high elevation (RG31; 1,363 m). Therefore, it was quite likely that soil moisture controls on Mid_{off} at low elevation regions were limited and temperature-related controls were more dominant.

The comparison of LAI_{max} between wet and dry years also supports that water availability is a more important limiting factor at lower elevation regions

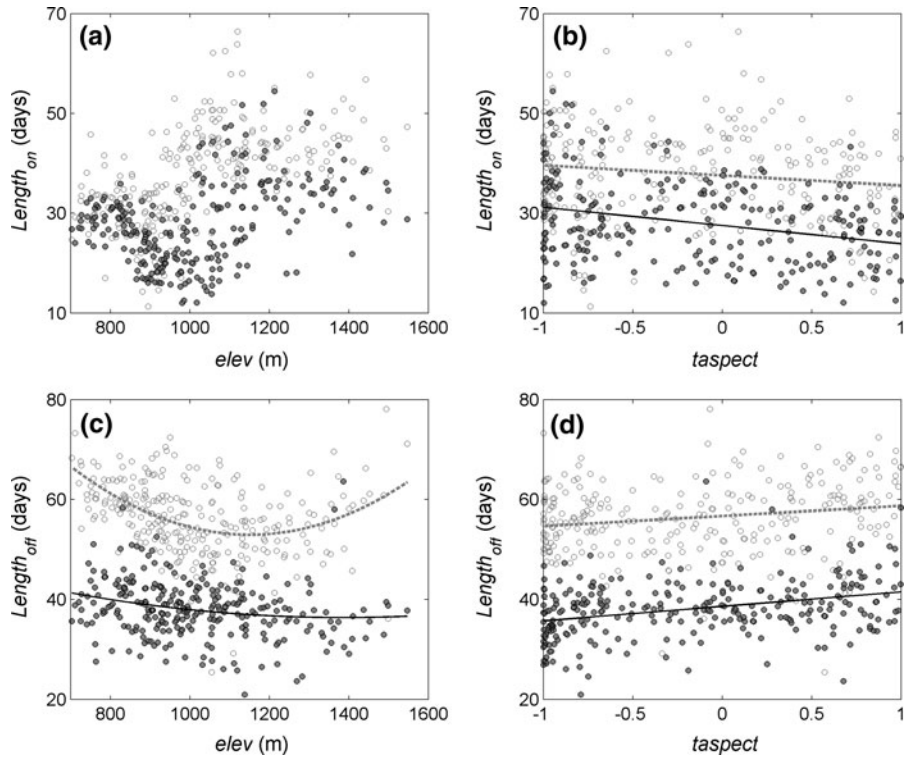

Fig. 8 Major topographic controls (*elev*, *taspect*) on two length phenological variables ($Length_{on}$, $Length_{off}$) between wet (*open circles* and *dashed fitted lines*) and dry years (*filled circles* and *solid fitted lines*)

(Fig. 7f). Greater increases of LAI_{max} in wet years are found in lower LAI_{max} ranges, usually developed at lower elevation regions (Fig. 5c). In addition, elevational controls on $Length_{off}$ between wet and dry years show higher increases in lower elevation regions (Fig. 8c). Vegetation in lower elevation regions is more sensitive to precipitation than mid-elevation regions, as water (or nitrogen) is a more critical factor for its growth. Recently, Vitasse et al. (2010) also reported similar quadratic responses of senescence for European beech (*Fagus sylvatica* L.) and sessile oak (*Quercus petraea*) in common garden experiments along the elevation gradient.

Temperature is still a dominant factor for other phenological variables in high elevation regions, represented as early litterfall, shorter greenup, and longer senescence period. Combined effects of temperature and water availability show distinct quadratic responses of three phenological variables along the elevation gradient, also associated with forest community type. High elevation regions are regarded as transition zones from the Southern Appalachian to the Northern Hardwoods forests (Fig. 2), which have different phenological responses to climate factors (Fisher et al. 2007). These patterns are also related to different limiting factors of vegetation growth along the elevational gradient; water or nitrogen at lower elevation regions and temperature at higher elevation regions (Knoepp et al. 2008).

Radiation controls on vegetation phenology

Radiation proxies are significant for all phenological variables (Table 3; Fig. 6), which convolves effects of potential radiation intensity and photoperiod, which are interannual invariant within topographic positions, and interannually varying temperature, vapor pressure deficit and water stress. Many studies have shown that photoperiod plays an important role in both greenup and senescence across different ecosystems (e.g. White et al. 1997; Partanen et al. 1998; Hakkinen et al. 1998). The controls of *taspect* on length phenological variables are consistent between wet and dry years (Fig. 8b, d), which may suggest photoperiod controls on vegetation phenology by radiation proxies. Photoperiods in this study represent topographically-modulated photosynthetic day length, which is related to the period between sunrise and sunset elevation angles.

In addition, radiation proxies have more explanatory power for Mid_{off} than Mid_{on} (Table 3). This is also supported by field measurements (Table 2). Longer photoperiods on south-facing slopes can delay Mid_{off} and lengthen $Length_{off}$. There is no common agreement on an appropriate model for leaf senescence, however some studies reviewed more dominant roles of photoperiod on senescence (or dormancy onset) than greenup (greenup onset or dormancy release) for cool and temperate woody plants (e.g. White et al. 1997, 2002; Vitasse et al. 2009). However, shorter $Length_{on}$ are also observed on south-facing slopes, hard to explain with photoperiod alone. In addition, radiation proxies also show weak negative relationships with Mid_{on} if the interaction terms with *elev* are included for both models (Table 3). They may represent faster growth of vegetation by combined effect of radiation and temperature, but more limited growth or greater belowground allocation resulting from water stress on south-facing slopes.

Other controls on vegetation phenology

Mid_{on} is slightly delayed with increase of *topidx*. This can be interpreted as delay of greenup in valley bottom positions, as a partial function of cold air drainage in complex terrain. Note that this is a function of terrain shape, and a departure from a simple linear elevation effect. Bolstad et al. (1998) found that the temperature lapse rates with elevation decreased in valley positions in this study area, attributed to cold air drainage. They also found that the reduced lapse rates were most pronounced in early spring, a period critical to greenup phenology, and lapse rates for minimum temperature in the valley were negative throughout the year because cold air drainage is predominant at night-time. Many studies show that minimum (or suboptimal) temperature is a stronger constraint on vegetation phenology across various ecosystems than either average or maximum temperature (e.g. Jarvis and Linder 2000; Jolly et al. 2005). Fisher et al. (2006) also reported a significant impact of cold air drainage on greenup phenology, a strong negative correlation between elevation and on-set date along four elevational transects in New England.

It is also possible that transitions to cove hardwoods species (e.g. *L. tulipifera*, *T. canadensis* and *A. rubrum* etc.) in cove regions (Fig. 2; Day et al. 1988) lead to unique sensitivity of Mid_{on} to *topidx*. However, it was also reported that there was no significant difference in greenup timing among five major deciduous species in the study area (Day and Monk 1974). Eastern hemlock (*T. canadensis*), one of the principal riparian and cove species, may have unique phenological patterns compared to broadleaf deciduous species. However, it is facing recent severe extirpation by the introduced insect (hemlock woolly adelgid) (Ford and Vose 2007), so it may have limited effect on observed phenological signals in this study.

Strong significant relationships of LAI_{min} with two mid-day phenological variables effectively represent the effect of coniferous and understory evergreen species on vegetation phenology (Table 3), characterized as delayed greenup and early senescence with higher LAI_{min}. Seasonal dynamics of pine LAI in this study area show typical sinusoidal patterns (Vose and Swank 1990). In addition, early developments of understory broadleaf may not be detected well by the sensor due to overstory evergreen vegetation in low NDVI ranges. This may also result in delayed greenup and early senescence in averaged phenological signals within a MODIS pixel.

Vegetation phenology under contemporary climate change

Vegetation phenology has been a major subject for global climate change research, as it shows seasonal patterns of canopy response to climate compared to long-term responses. This study reveals possible phenological responses to near-future climate change in the Southern Appalachian forests. The dominant effect of temperature on the greenup phenology implies that temperature increase will advance the start of spring. Recent warming in the southeast USA is better manifested in daily minimum temperatures than maximum (Band and Salvesen 2009). We can estimate how the start of spring may advance with unit increase of the daily minimum temperature from the average minimum temperature lapse rate around this region (about 0.3°C/100 m; Bolstad et al. 1998) and the Mid_{on} sensitivity with elevation in this study (about 3.4 days/100 m).

However, the elevational control on senescence indicates that temperature increases may have less

uniform effect on senescence especially in low elevation regions where water availability is also a critical factor for senescence. Temperature increases instead may exacerbate plant water stress due to potential evapotranspiration increases. This may also result in shifting the inflection point of Mid_{off} into higher elevations (Fig. 5a). This projected phenological shift suggests the ecotone region between the Northern Hardwood and the Southern Appalachian forests may move toward higher elevation region and the xeric oak-pine community types will dominate in lower elevation region in the long term (Fig. 2).

Many researchers have stated that senescence does not respond to temperature increase as strongly as greenup (e.g. Myneni et al. 1997; Chen et al. 1999; Black et al. 2000; Menzel et al. 2006), although there are several counter examples (e.g. Menzel and Fabian 1999; Zhou et al. 2001). This study suggests that senescence is more affected by photoperiod and plant water stress than greenup phenology even in humid temperate forests. In this sense, this study may provide an explanation for the lack of a consistent trend in senescence compared to greenup phenology with global climate change.

Conclusions

In this study, we extract phenological signals from 8-year MODIS NDVI (2001–2008) and 1-year field measurements (1989) within the Coweeta LTER site. These phenological signals are related to topographic variables. Elevation shows strong linear or quadratic relationships with four phenological variables. Quadratic responses of three phenological variables (Mid_{off}, $Length_{on}$, and $Length_{off}$) with elevation are explained by combined effects of temperature and water availability along the elevation gradient. Radiation proxies (*taspect* and *PRRs*) also have explanatory power for phenological variables, mostly associated with photoperiod controls on vegetation phenology. The hillslope position (*topidx*) shows a significant effect on the Mid_{on} variable, possibly related to decreased temperature lapse rates along local hillslope gradients by cold air drainage. Though topographic wetness position at 250-m resolution is not observed to have a significant effect on vegetation phenology from MODIS NDVI, the difference in vegetation phenology between extremely wet and dry years suggests extended greenup and senescence in wet years. These topography-mediated phenological patterns are strongly supported by field PAR transmittance measurements at different topographic positions within the study area. In conclusion, topography-mediated controls on local vegetation phenology are closely related to the combined effect of microclimate variations, vegetation community type, and water availability. The capability of detecting the topography-mediated local phenology offers the potential to detect vegetation responses to near-future global climate change in mountainous terrain.

Acknowledgments This research was supported by the National Science Foundation award to the Coweeta Long Term Ecologic Research project (DEB #0823293). We thank two anonymous reviewers and the editor for constructive comments which improved the quality of this manuscript substantially.

References

Angert A, Biraud S, Bonfils C, Henning CC, Buermann W, Fung I (2005) Drier summers cancel out the CO_2 uptake enhancement induced by warmer springs. Proc Natl Acad Sci USA 102:10823–10827

Band LE, Salvesen D (2009) Climate Change Committee Report. Institute for the Environment, University of North Carolina at Chapel Hill. http://www.ie.unc.edu/PDF/Climate_Change_Report.pdf

Beers TW, Dress PE, Wensel LC (1966) Aspect transformation in site productivity research. J For 64:691–692

Beven K, Kirkby M (1979) A physically-based variable contributing area model of basin hydrology. Hydrol Sci Bull 24:43–69

Black TA, Chen WJ, Barr AG, Arain MA, Chen Z, Nesic Z, Hogg Z, Neumann HH, Yang PC (2000) Increased carbon sequestration by a boreal deciduous forest in years with a warm spring. Geophys Res Lett 27:1271–1274

Bolstad PV, Swift L, Collins F, Regniere J et al (1998) Measured and predicted air temperatures at basin to regional scales in the southern Appalachian mountains. Agric For Meteorol 91:161–176

Chen WJ, Black TA, Yang PC, Barr AG, Neumann HH, Nesic Z, Blanken PD, Novak MD, Eley J, Ketler RJ, Cuenca R (1999) Effects of climatic variability on the annual carbon sequestration by a boreal aspen forest. Global Change Biol 5:41–53

Churkina G, Schimel D, Braswell BH, Xiao XM (2005) Spatial analysis of growing season length control over net ecosystem exchange. Global Change Biol 11:1777–1787

Day FP, Monk CD (1974) Vegetation patterns on a southern Appalachian watershed. Ecology 55:1064–1074

Day FP, Philips DL, Monk CD (1988) Forest communities and patterns. In: Swank WT, Crossley JDA (eds) Forest hydrology and ecology at Coweeta. Springer-Verlag, New York, NY, USA, pp 141–149

Didan K, Huete A (2006) MODIS vegetation index product series collection 5 change summary. TBRS Lab, The University of Arizona

Fisher JI, Mustard JF, Vadeboncoeur MA (2006) Green leaf phenology at landsat resolution: scaling from the field to the satellite. Remote Sens Environ 100:265–279

Fisher JI, Richardson AD, Mustard JF (2007) Phenology model from surface meteorology does not capture satellite-based greenup estimations. Global Change Biol 13:707–721

Ford CR, Vose JM (2007) *Tsuga canadensis* (L.) Carr. mortality will impact hydrologic processes in southern Appalachian forest ecosystems. Ecol Appl 17:1156–1167

Hakkinen R, Linkosalo T, Hari P (1998) Effects of dormancy and environmental factors on timing of bud burst in Betula pendula. Tree Physiol 18:707–712

Hopkins AD (1918) Periodical events and natural law as guides to agricultural research and practice. Mon Weather Rev 9(Suppl.):1–42

Huete A, Didan K, Miura T, Rodriguez EP, Gao X, Ferreira LF (2002) Overview of the radiometric and biophysical performance of the MODIS vegetation indices. Remote Sens Environ 83:195–213

Jarvis P, Linder S (2000) Constraints to growth of boreal forests. Nature 405:904–905

Jolly WM, Nemani R, Running SW (2005) A generalized, bioclimatic index to predict foliar phenology in response to climate. Global Change Biol 11:619–632

Keeling CD, Chin JFS, Whorf TP (1996) Increased activity of northern vegetation inferred from atmospheric CO_2 measurements. Nature 382:146–149

Knoepp JD, Vose JM, Swank WT (2008) Nitrogen deposition and cycling across an elevation and vegetation gradient in southern Appalachian forests. Int J Environ Stud 65:389–408

Lovell JL, Graetz RD (2001) Filtering pathfinder AVHRR land NDVI data for Australia. Int J Remote Sens 22:2649–2654

Menzel A, Fabian P (1999) Growing season extended in Europe. Nature 397:659

Menzel A, Sparks TH, Estrella N, Koch E, Aasa A, Ahas R, Alm-Kubler K, Bissolli P, Braslavska O, Briede A, Chmielewski FM, Crepinsek Z, Curnel Y, Dahl A, Defila C, Donnelly A, Filella Y, Jatczak K, Mage F, Mestre A, Nordli O, Penuelas J, Pirinen P, Remisova V, Scheifinger H, Striz M, Susnik A, Van Viet AJH, Wielgolaski F-E, Zach S, Zust A (2006) European phenological response to climate change matches the warming pattern. Global Change Biol 12(10):1969–1976

Myneni RB, Keeling CD, Tucker CJ, Asrar G, Nemani RR (1997) Increased plant growth in the northern high latitudes from 1981 to 1991. Nature 386:698–702

Myneni RB, Hoffman S, Knyazikhin Y, Privette JL, Glassy J, Tian Y, Wang Y, Song X, Zhang Y, Smith GR, Lotsch A, Friedl M, Morisette JT, Votava P, Nemani RR, Running SW (2002) Global products of vegetation leaf area and fraction absorbed PAR from year one of MODIS data. Remote Sens Environ 83:214–231

Partanen J, Koski V, Hanninen H (1998) Effects of photoperiod and temperature on the timing of bud burst in Norway spruce (Picea abies). Tree Physiol 18:811–816

Pierce KB, Lookingbill T, Urban D (2005) A simple method for estimating potential relative radiation (PRR) for landscape-scale vegetation analysis. Landscape Ecol 20:137–147

Richardson AD, Bailey AS, Denny EG, Martin CW, O'Keefe J (2006) Phenology of a northern hardwood forest canopy. Global Change Biol 12:1174–1188

Swift LW, Cunningham JGB, Douglass JE (1988) Climatology and hydrology. In: Swank WT, Crossley JDA (eds) Forest hydrology and ecology at Coweeta. Springer-Verlag, New York, NY, USA, pp 35–55

Tarboton DG (1997) A new method for the determination of flow directions and upslope areas in grid digital elevation models. Water Resour Res 33:309–319

Vitasse Y, Porte AJ, Kremer A, Michalet R, Delzon S (2009) Responses of canopy duration to temperature changes in four temperate tree species: relative contributions of spring and autumn leaf phenology. Oecologia 161:187–198

Vitasse Y, Bresson CC, Kremer A, Michalet R, Delzon S (2010) Quantifying phenological plasticity to temperature in two temperate tree species. Funct Ecol 24:1211–1218

Vose JM, Swank WT (1990) Assessing seasonal leaf-area dynamics and vertical leaf-area distribution in eastern white-pine (*Pinus-Strobus* L) with a portable light-meter. Tree Physiol 7:125–134

White MA, Nemani AR (2003) Canopy duration has little influence on annual carbon storage in the deciduous broad leaf forest. Global Change Biol 9:967–972

White MA, Thornton PE, Running SW (1997) A continental phenology model for monitoring vegetation responses to interannual climatic variability. Glob Biogeochem Cycles 11:217–234

White MA, Nemani RR, Thornton PE, Running SW (2002) Satellite evidence of phenological differences between urbanized and rural areas of the eastern United States deciduous broadleaf forest. Ecosystems 5:260–273

Whittaker RH (1956) Vegetation of the great smoky mountains. Ecol Monogr 26:1–69

Zhang XY, Friedl MA, Schaaf CB, Strahler AH (2004) Climate controls on vegetation phenological patterns in northern mid- and high latitudes inferred from MODIS data. Global Change Biol 10:1133–1145

Zhang XY, Friedl MA, Schaaf CB (2006) Global vegetation phenology from moderate resolution imaging spectroradiometer (MODIS): evaluation of global patterns and comparison with in situ measurements. J Geophys Res Biogeosci 111:G04017

Zhou LM, Tucker CJ, Kaufmann RK, Slayback D, Shabanov NV, Myneni RB (2001) Variations in northern vegetation activity inferred from satellite data of vegetation index during 1981 to 1999. J Geophys Res Atmos 106:20069–20083